

## Numerical and experimental studies of a building with roller seismic isolation bearings

Nelson A. Ortiz<sup>\*</sup>, Carlos Magluta<sup>a</sup> and Ney Roitman<sup>b</sup>

*Department of Civil Engineering, COPPE/UFRJ Centro de Tecnologia, Bloco I2000, Sala I116, Cidade Universitária, Ilha do Fundão, Rio de Janeiro, CEP21945-970, Brazil*

*(Received October 24, 2013, Revised November 12, 2014, Accepted December 27, 2014)*

**Abstract.** This study presents the validation of a numerical model developed for dynamic analysis of buildings with roller seismic isolation bearings. Experimental methods allowed validation of the motion equations of a physical model of a building with and without roller bearings under base excitation. The results are presented in terms of modal parameters, frequency response functions (FRFs) and acceleration response. The agreement between numerical and experimental results proves the accuracy of the developed numerical model. Finally, the performance of the constructed seismic protection system is assessed through a parametric study.

**Keywords:** base isolation systems; seismic protection systems; frequency response functions; roller seismic isolation bearings

---

### 1. Introduction

In the last decade, base isolation systems have proved to be very efficient in building seismic protection. Important applications have been developed in countries with higher occurrence of earthquakes. The success of base isolation systems is due to their reliability, stability, simplicity of design and low cost when compared to other methodologies, Spencer (2003). These systems also allow the retrofitting of existing structures with insufficient resistance to withstand earthquakes.

In general, seismic base isolation systems are intended to partially decouple the horizontal components of ground movement by placing elements with low lateral stiffness between the structure and its foundation.

According to Datta and Jangid (1995), the main concept of base isolation is the reduction of structure fundamental frequency to a lower value than the frequencies contained in the predominant energy of a seismic excitation. In this condition, a significant reduction of the structure dynamic response is expected. A base isolation system can also be considered a mechanical filter whose effectiveness depends on the frequency filtering capacity where the energy of the earthquake is prevalent and closer to the fundamental frequencies of the structure.

---

\*Corresponding author, D.Sc. Student, E-mail: nelkano@gmail.com

<sup>a</sup>Professor, E-mail: magluta@coc.ufrj.br

<sup>b</sup>Professor, E-mail: roitman@coc.ufrj.br

According to Palazzo (1999), the filtering effect mainly influences the inter-story drifts of a structure, while large deformations are contained in the isolation bearing.

A great variety of isolation systems has been proposed to protect buildings and bridges from seismic excitation. These systems are frequently classified into three groups: (i) elastomeric bearings, (ii) sliding bearings that use a friction mechanism to isolate seismic excitation and (iii) roller bearings through cylinders and spheres, characterized by a rolling friction coefficient significantly lower than the sliding friction coefficient.

A wide review of these systems was presented by Jangid and Datta (1995), Kunde and Jangid (2003), Lee (2007). Other systems with very particular characteristics, such as an elastomeric bearing with shape-memory alloy studied by Gur *et al.* (2013) and a magneto-rheological elastomeric bearing developed by Li *et al.* (2013), have certainly expanded the frontiers of base isolator applications.

The main objective of this study is to experimentally validate a numerical model for buildings with roller seismic isolation bearings. Validation of the numerical model allows assessment of the performance of the isolator in earthquake excitations. The system proposed by Lee (2010), composed of rollers and sloping surfaces, was initially studied and applied to bridges; however, in this study, the system is used in multicolumn systems such as buildings.

The experimental methodologies of analysis used in the validation and characterization of different systems are discussed in this paper. Numerical models of buildings with and without roller isolation bearings are calibrated by modal identification and laboratory tests. Finally, the performance of the isolation systems is assessed through a parametric study using earthquake records.

## 2. Theoretical basis of buildings under seismic excitation

The dynamic models of structural systems were obtained through the finite element method (FEM). The columns of a building (B) with  $n$  floors were discretized in frame elements whose mechanical and geometric properties are defined by the modulus of elasticity  $E$ , the moment of inertia  $I$ , the section area  $A$ , and the specific weight of the material  $\rho$ . The mass of each floor was simulated by concentrated masses  $m_b, m_1, m_2 \dots m_n$ , located at heights  $h_0, h_1, h_2 \dots h_n$ , as shown in Fig. 1. Additionally, flexure springs  $k_\beta$  were considered to partially inhibit rotation of each building level. A structure with linear behavior was assumed, with nonlinearities caused by the isolation system adopted.

The seismic isolation of roller bearings (RB) is characterized by the restoring force  $f_s$ , the angle  $\theta$  of the bearing sloping surface and the friction coefficients  $\mu_s$  and  $\mu_r$  for sliding and rolling, respectively. Fig. 1 presents a dynamics model of the building with roller bearings (B+RB).

The motion equation for the building with RB under seismic excitation ( $u_g$ ) that is shown in Fig. 1 is written as

$$M\ddot{u} + C\dot{u} + Ku + R(f_s + f_{Dr} + f_{Ds}) = -M\Gamma\ddot{u}_g \quad (1)$$

where  $M$ ,  $C$ , and  $K$  are the mass, damping and stiffness matrices, respectively, while  $\ddot{u}$ ,  $\dot{u}$  and  $u$  are vectors that store acceleration, velocity and displacement of the multi-degrees-of-freedom system (MDOF). The term  $\Gamma$  is the influence coefficient vector that relates the excited degrees of freedom (DOF) according to the direction of seismic excitation  $\ddot{u}_g$ . The dimension of this

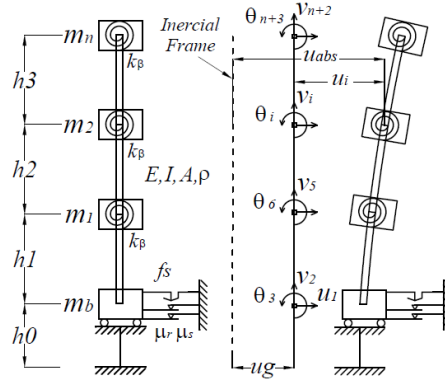


Fig. 1 Building with roller isolation bearings under seismic excitation

coefficient depends on the number of excitations used. Thus, the coefficient has as many columns as acceleration components are applied, and their elements take values equal to 1 for the DOF that correspond to the direction of the  $\ddot{u}_g$  seismic excitation and zero for the other degrees of freedom. The vector  $R$  defines the position of the restoring force  $f_s$ , rolling friction  $f_{Dr}$  and sliding friction  $f_{Ds}$  developed in the RB system.

The stiffness matrix of the B+RB is non-singular, conducting to null frequencies in the eigenvalue problem; however, it is possible to solve the system by applying the restoring and friction forces in the base DOF through vector  $R$ . The restoring and friction forces are described by Eqs. (2)-(4)

$$f_s = 0.5m_t g \sin \theta Sng(u_b) \tag{2}$$

$$f_{Dr} = \mu_r m_t g Sng(\dot{u}_b) \tag{3}$$

$$f_{Ds} = \mu_s N Sng(\dot{u}_b) \tag{4}$$

where  $\mu_s$  is the sliding coefficient,  $N$  is the normal force applied to the sliding interface, and  $g$  is acceleration due to gravity. The  $Sng(\cdot)$  function was substituted with Eq. (5), where  $d$  represents “yield” displacement,  $k_y$  “yield” stiffness and  $y$  is an auxiliary variable.

$$f_1(y) = \begin{cases} 1 & sey > d \\ k_y y se - d < y < d \\ -1 & sey < -d \end{cases} \tag{5}$$

To solve the motion equation for the variable step-size Runge Kutta method, Eq. (1) must be re-written in the form of a state equation

$$\dot{x}(t) = A_1 x(t) + A_2 H(u_b, \dot{u}_b) + A_3 \ddot{u}_g \tag{6}$$

$$A_1 = \begin{bmatrix} 0 & I \\ -M^{-1}K & -M^{-1}C \end{bmatrix} \quad A_2 = \begin{bmatrix} 0 \\ M^{-1}R \end{bmatrix} \quad A_3 = \begin{bmatrix} 0 \\ -M\Gamma \end{bmatrix} \tag{7}$$

The terms  $A_1$  and  $x(t) = [u \ \dot{u}]^T$  represent the state matrix and state vector of the system. The nonlinearity of Eq. (6) is represented by  $H(u_b, \dot{u}_b)$ , which contains the effects of the friction

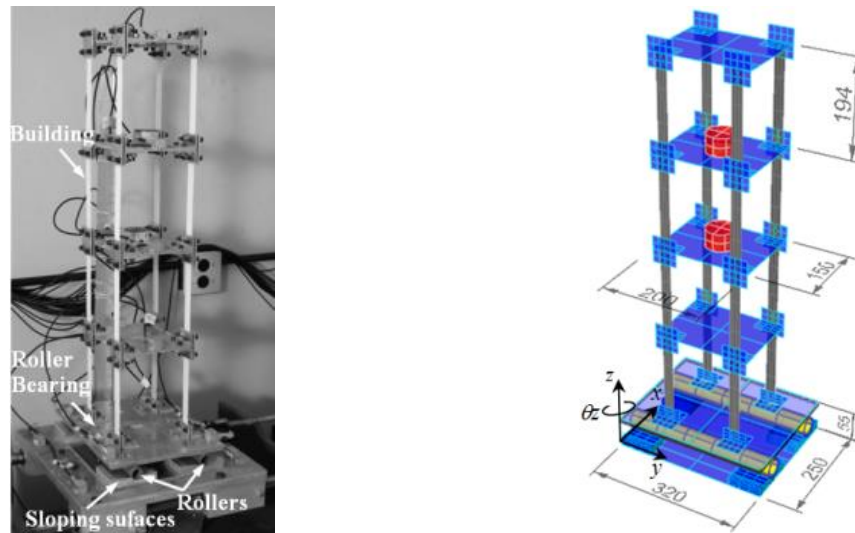


Fig. 2 Physical model of a building with roller isolation bearings , measures in (mm)

mechanism described above. In the construction of matrix  $C$ , classical Rayleigh damping was considered. Initially, the Runge Kutta classical method was used in the integration of Eq. (6) but brought serious problems of numeric instability, convergence and high computation costs. Thus, the TR-BDF implicit integration algorithm (Shampine 1996) was used to solve the motion equation. This algorithm is available for Matlab users through the ode23tb integrator.

### 3. Experimental methods of analysis

#### 3.1 Description of the building physical model

A building physical model was constructed at the Laboratory of Dynamics Analysis and Image and Signal Processing (LADEPIS) from COPPE-UFRJ (Alberto Luiz Coimbra Institute of Federal University of Rio de Janeiro) to validate the motion equations of buildings under base excitation with and without roller seismic isolation bearings.

Fig. 2 presents the building physical model, which is a four-story frame supported by four columns. The floors were 4.0-mm-thick aluminum plates, and the columns were polymer blades. The average story height is 194 mm. The columns had a  $20 \times 2.94$  mm cross-section and were fixed to each floor through aluminum connectors. In addition, two 0.50-kg masses were considered on the second and third floors. The objective of these masses was to separate the torsional modes from the bending modes, which are the focus of the present study.

A  $320 \times 250$  mm aluminum plate was placed at the base of the frame to fix the frame to the excitation and RB seismic isolation systems.

To determine the elasticity modulus of the column material, bending stiffness tests were performed in a simply supported beam with a 50-cm span. A displacement sensor was placed in the beam, at an 8-cm distance from one of the supports, and loads were imposed in the middle of the span with known weights. The test was performed ten times to verify the repeatability of the

Table 1 Modal parameters identified in the fixed-base building

Mode	$f_{exp}(Hz)$	$f_{num}(Hz)$	$\zeta_{exp}(\%)$	$\zeta_{num}(Hz)$
1	6.82±0.02	6.82	0.59±0.03	0.59
2	20.44±0.03	20.43	0.52±0.01	0.51
3	31.70±0.02	31.74	0.30±0.01	0.66
4	36.65±0.03	37.01	0.34±0.02	0.74

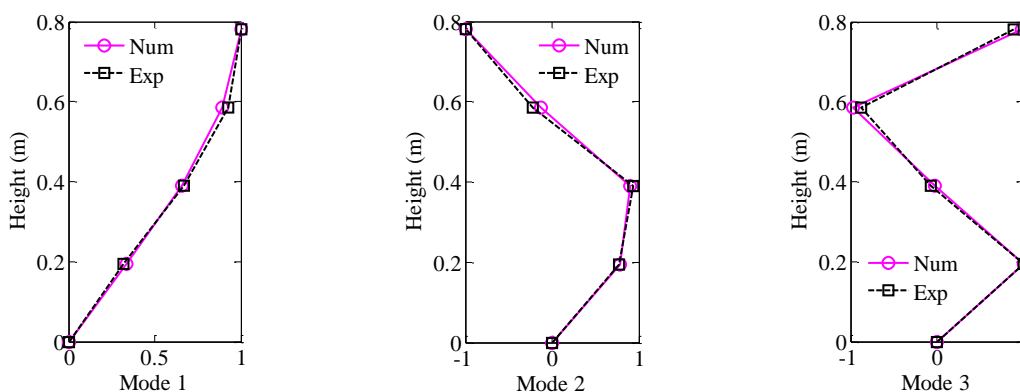


Fig. 3 Vibration modes identified

measures, obtaining standard deviations less than 4%. A mean value of 31 GPa was estimated for the elasticity modulus and used as a reference in the calibration of the building numerical model.

### 3.2 Identification of modal parameters

To estimate the modal parameters, modal identification tests were conducted. These tests allowed identification of the flexural vibration modes in the  $x$  direction, indicated in Fig. 2. During the tests, the base was locked to ensure that only the frame was vibrating.

The frame was excited with impacts on the first floor, and the response was measured by acceleration sensors placed on the floors of the building in the  $x$  direction. The data acquisition system was composed of sensors, signal conditioners and an acquisition board installed in a PXI NI computer. The system used samples of 516 s (8.6 min) with a time interval of 0.002 s (500-Hz sampling frequency).

The modal parameters were determined from the time series measured using the Short Time Fourier Transform (STFT) method, the implementation of which was performed by Bucher (2001). Taking into consideration the modal parameters estimated in each impact, the mean values and standard deviations of the natural frequencies and damping ratios were obtained. The modal parameters experimentally and numerically obtained through the equations of motion presented in the above section are shown in Table 1. The following properties were assumed in the numerical modeling process:  $E = 65.4 \text{ GPa}$ ,  $I = 19.74 \times 10^{-11} \text{ m}^4$ ,  $A = 2.54 \times 10^{-4} \text{ m}^2$ ,  $\rho = 1800 \text{ Kg/m}$ ,  $k_\beta = 7.5 \times 10^4 \text{ Nm/rad}$ , concentrated masses  $m_b = 2.2 \text{ kg}$ ,  $m_1 = 1.023 \text{ kg}$ ,  $m_2 = 1.5217 \text{ kg}$ ,  $m_3 = 1.5213 \text{ kg}$  and heights between floors  $h_1 = 0.1923 \text{ m}$ ,  $h_2 = 0.1946 \text{ m}$ ,  $h_3 = 0.1949 \text{ m}$ ,  $h_4 = 0.1942 \text{ m}$ . The adjusted value of the elasticity modulus is approximately twice the value obtained experimentally by a flexural test of the simple element, which is primarily due to the size

of floor connections that increased the lateral stiffness of columns.

This table shows excellent agreement between the experimental and numerical frequencies, but there is divergence in the damping ratios of the third and fourth vibration modes.

Fig. 3 shows an experimental and numerical comparison between the first three vibration modes. The experimental mode shapes were obtained from the phases and spectra of the acceleration response. The excellent correlation confirms that the numerical model accurately represents the dynamic behavior of the building physical model.

The results of modal parameter identification were confirmed through a set of FRFs, estimated through the building floor acceleration and the force imposed by a hammer. A Hamming-type window with 65% series overlapping was chosen to estimate the FRFs, and the number of samples was always higher than 100.

With the exact location of the output and excitation points, the FRFs of the building were estimated. A comparison of the fourth-floor FRFs of the building is shown in Fig. 4. In this figure, the resonance amplitudes correspond to the first, second and third bending modes of the building. The frequencies of these amplitudes are practically the same as the results shown in Table 1, further demonstrating that the numerical model efficiently represents a physical four-story building model. A comparison of the FRFs of the remaining floors presented similar results to those indicated in Fig. 4.

Finally, the numerical model was verified in the time domain. The response to a random excitation imposed in the base was obtained through numerical integration of the fixed-base building motion. Fig. 5 presents a comparison of the calculated response in terms of acceleration and the experimentally measured response.

Similar results were found in the remaining building floors. The excellent correlation of these

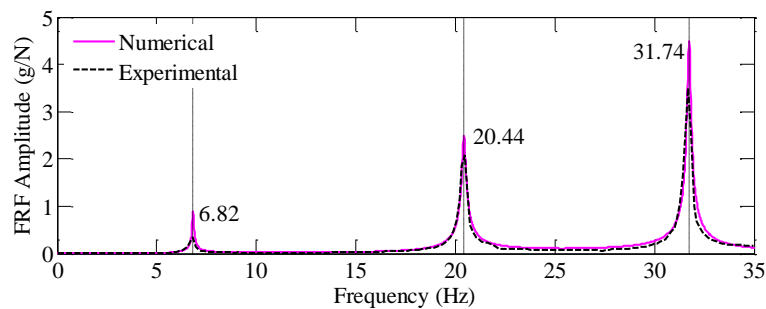


Fig. 4 Comparison of the FRFs of the building's fourth floor

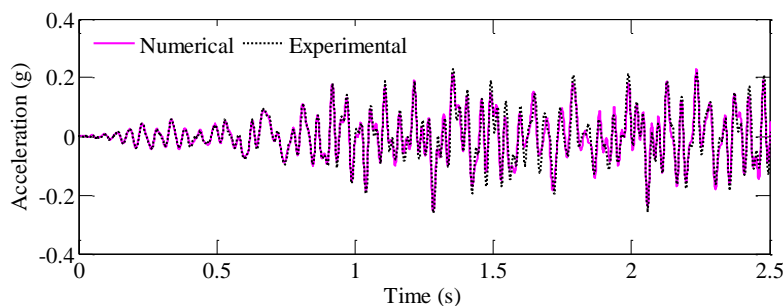
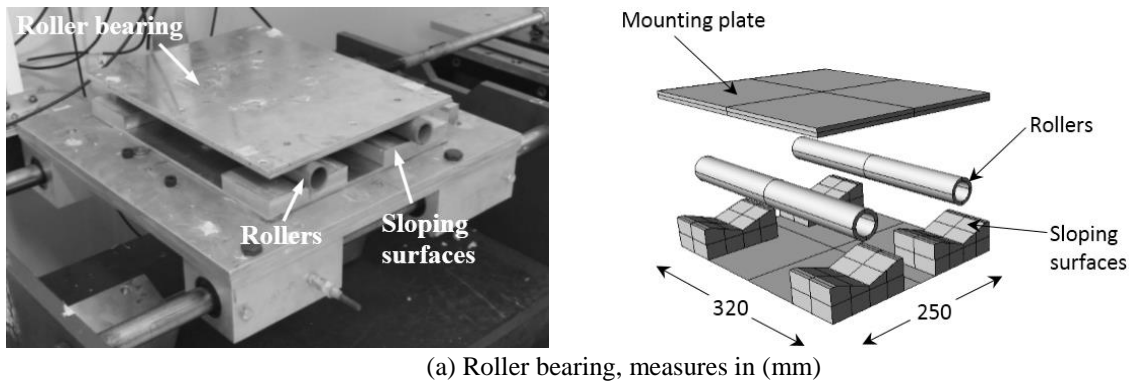
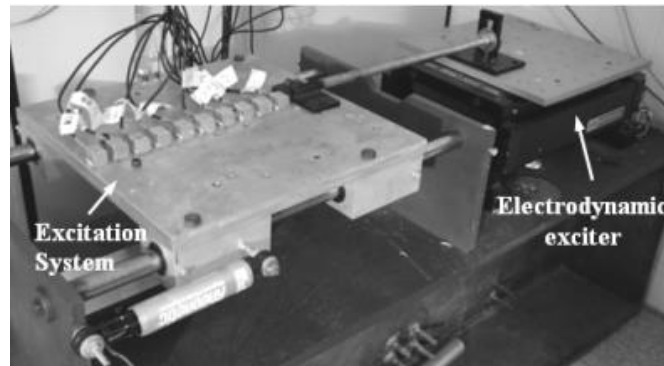


Fig. 5 Acceleration response of second story



(a) Roller bearing, measures in (mm)



(b) Excitation system

Fig. 6 Seismic isolation and excitation systems

results indicates the adequate representation of the building physical model. Before correlating the numerical results of the B+RB system, the main parameters of the roller bearing were identified.

#### 4. Base isolation systems

To reduce the building dynamic response in terms of building story accelerations and shear forces, a roller seismic isolation bearing was constructed as shown in Fig. 6(a). The roller bearings were composed of PVC rollers and aluminum sloping surfaces. The slopes of the surfaces allow the development of a restoring force that returns the system to its initial conditions.

The RB was composed of aluminum plates that facilitated coupling with the building physical model and the excitation system (Fig. 6(b)). This section presents the characterization of the proposed isolation system. The identified parameters are essential for the calibration of the building numerical model associated with earthquake isolation systems. To identify the main parameters ( $f_s, \mu_r$ ) of the roller bearing, an experimental program of seismic isolation systems was conducted.

##### 4.1 Restoring force, $f_s$ , and friction coefficient, $\mu_r$

Recently, isolation systems based on roller bearing systems have been intensively studied.



Fig. 7 Tests for the characterization of the restoring force of the RB

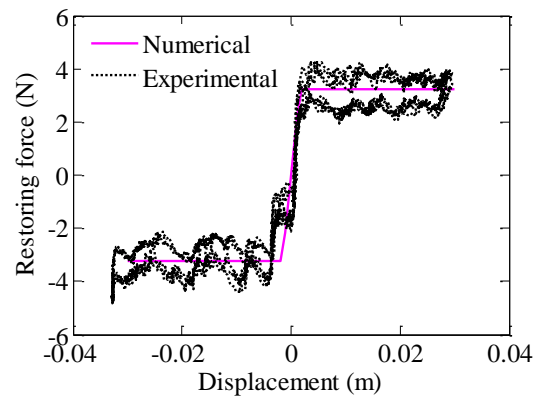


Fig. 8 Restoring force  $f_s$  of the RB supporting an equivalent mass

Authors such as Lin *et al.* (1995), Jangid and Londhe (2000), Chung *et al.* (2009), Ou (2010) have indicated the benefits of these systems in the seismic protection of structures. The main advantage of roller bearing systems compared to other methodologies such as friction pendulum bearing systems is that, generally, the rolling friction resistance is significantly lower than the sliding friction resistance, which allows efficient separation of the seismic excitation of the structure.

In this context, a roller bearing isolation system was constructed to be installed in the building physical model. The system was composed of two PVC rollers with the following geometric properties: length  $L = 0.340\text{m}$ , diameter  $\varphi = 0.0254\text{ m}$  and thickness  $t = 0.0026\text{ m}$ . The rollers had a mass of  $m_r = 84.67\text{ g}$ , and their motion occurred on aluminum sloping surfaces with a five-degree slope ( $\theta=5^\circ$ ). The displacement capacity of the bearing was 70 mm.

An important parameter in RB characterization is the restoring force ( $f_s$ ), the behavior of which is nonlinear. This force is composed of an elastic force proportional to the displacement and a constant maximum force. The elastic force develops when the rollers are in the transition region between sloping surfaces, while the constant force is associated with the movement of the roller on the sloping surface.

To characterize the RB restoring force, experimental tests were performed, measuring the displacement of the system due to an imposed force on the bearing. The test assemblage was

composed of an LVDT and a load cell, as shown in Fig. 7. The system was manually moved from right to left and vice versa, while the sensors recorded the measurements of each cycle. The characterization was performed in two ways, with a mass (7.58 kg) approximately equal to the mass of the structure (Fig. 7(a)) and the frame structure (Fig. 7(b)).

Fig. 8 shows the variation of force with displacement of the system with an equivalent mass. This figure also shows the numerical restoring force calculated by Eq.(2). The nonlinear behavior of  $f_s$  mentioned above can be observed in this figure.

Calibration of the theoretical curve was accomplished through the parameter  $d$ , which defines the interval of elastic behavior of the system. Satisfactory results in the comparison of force  $f_s$  were obtained, assuming a displacement  $d = 1.20$  mm. This value is in accordance with the typical values of 1 to 1.5 mm reported by Lee (2010). However, assuming a slope  $\theta = 5^\circ$  in Eq. (2), a maximum restoring force of 3.2 N was estimated in the bearing, which is very close to the experimental value. The good agreement between theoretical and experimental results indicates that the developed system of roller bearings is adequate to be installed in the physical model of the proposed building.

The rectangular shape of the experimental curve is due to the rolling friction force  $f_{Dr}$ . Thus, free-vibration (FV) tests were performed to estimate the rolling friction coefficient  $\mu_r$ . The FV test consists of pulling and suddenly releasing the top fixation plate of the system. Sensors disposed in the bearing allowed measurement of the RB acceleration response.

However, assuming a system with one DOF without energy dissipation, in FV conditions with initial displacement of 35 mm and zero initial speed, and representing the function  $Sng(\cdot)$  by a continuous function  $f_1(x)$  defined through the parameter  $d = 1.20$  mm, Eq. (6) was solved using the Runge Kutta 4th-order method. The value of coefficient  $\mu_r$  was estimated using a trial-and-error procedure that attempted to match the numerical and experimental responses. Assuming a value of  $\mu_r = 0.005$ , very satisfactory results were obtained, as shown in Fig. 9. Despite the good agreement between the results, small phase differences were observed between the responses, especially at the intersection point of the sloping surfaces, which are probably due to imperfections associated with the warping of aluminum plates and PVC rollers. These imperfections cause clearances on the system that make it unstable. Better finishing of the plates and rollers, together with a smoothing of the vertex, would be sufficient to limit that clearance and improve their behavior.

Values of rolling friction coefficients  $\mu_r$  are scarce; however, the coefficient can be calculated based on the expressions presented by Avallone and Baumeister (2007). Thus, assuming that the contact surfaces are made of steel and considering a roller diameter  $\varphi_r = 25$  mm, the coefficient

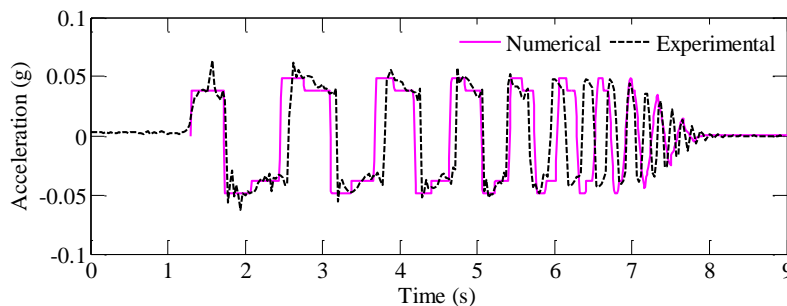


Fig. 9 Acceleration response of the RB system in Free Vibration Tests

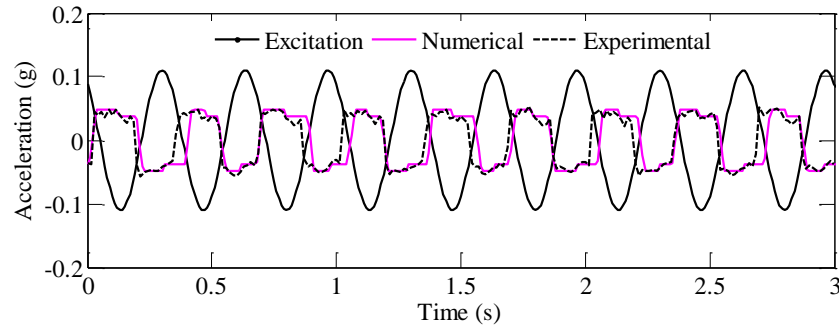


Fig. 10 Accelerations response of the RB in Forced Vibrations Tests

$\mu_r = 0.004$  was obtained. Comparing this value with the coefficient estimated in the experimental test ( $\mu_r = 0.005$ ), we conclude that the identified value is adequate and therefore can be used in the correlation results of the RB system.

To validate the parameters identified in this section, the RB system was tested in forced-vibration (FoV) conditions. To this end, harmonic excitations with 3-Hz frequency and  $A = 0.11$  g amplitude were imposed to the system. Sensors placed on the excitation system and the RB allowed measurement of the acceleration response of the bearing.

Considering the parameters identified in the FV tests and solving Eq. (5), RB acceleration responses due to harmonic base excitation were obtained. Fig. 10 presents a comparison of the typical response accelerations obtained numerically and experimentally. The excellent agreement of these results confirms the adequate representation of the roller bearing system. Notably, the RB responds with a maximum acceleration of approximately 0.05 g. This value was expected according to previous studies.

## 5. Correlation and parametric study

### 5.1 Building with seismic isolation bearings

To validate the numerical model of the B+RB system, free-vibration and base-excitation tests were conducted on the physical building equipped with roller bearing isolation.

The first test consisted of pulling and releasing the base of the B+RB system. Acceleration sensors placed at the different levels of the building and a NI PXI DAQ platform allowed measurement of the B+RB response.

The accelerations measured were correlated with those obtained through numerical simulations of the B+RB system. Considering the properties of the building and assuming initial conditions of displacement and acceleration ( $u_0 = 0.025$  m,  $\dot{u}_0 = 0$ ), acceleration responses were obtained using the Matlab `@ode45tb` integrator. Additionally, the following isolator parameters were assumed in the model:  $\mu_r = 0.0054$ ,  $d = 1.20$  mm, and  $\theta = 5^\circ$ . These parameters are notably almost the same as the values obtained in FV tests of the roller bearing supporting an equivalent mass of the building. Small differences in the coefficient  $\mu_r$  are probably associated to imperfections of the system, mainly warping of bearing rollers and plates or the discontinuity of the vertex of the slope surfaces.

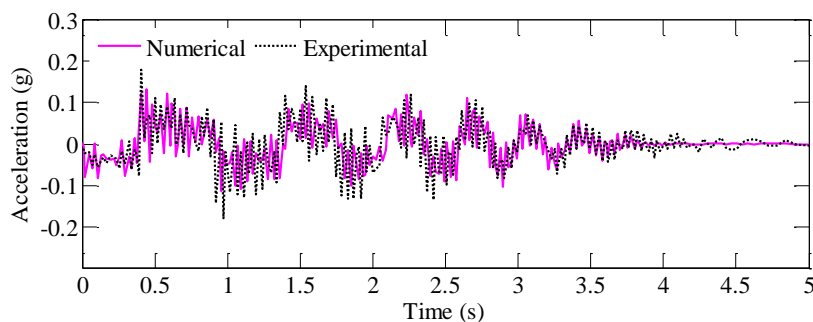


Fig. 11 Acceleration response of the B+RB system in Free Vibration Tests

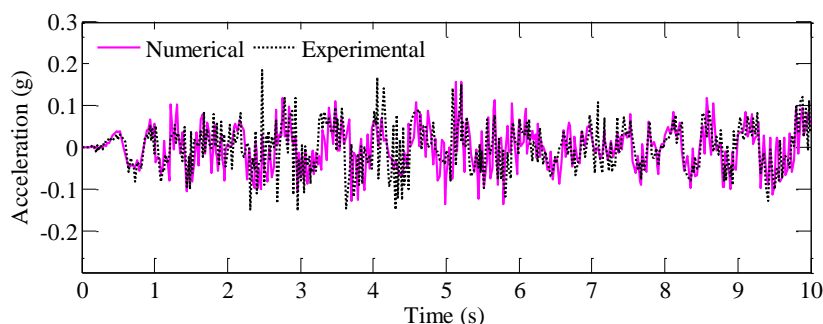


Fig. 12 Acceleration response of the B+RB system in Random Forced Tests

Based on the high correlation among acceleration responses (Fig. 11), we can conclude that the identified parameters are adequate and can be considered in the seismic analysis of B+RB systems. In this context, the system was excited through random functions in the frequency range of 0-6 Hz. This range was selected such that the base displacements were greater than the transition interval defined by  $d$ .

Similar to the FV test, acceleration responses were obtained via the base-excitation test. To correlate these results, motion equations were solved assuming the building properties and parameters identified in the FV test. Fig. 12 presents the correlation between measured and calculated acceleration responses.

From this figure, there is a certain degree of dispersion in the results; however, the correlation is quite satisfactory. The dispersion is probably associated with rotational movement of the building base observed in the tests. These movements become an unstable system and allow the emergence of torsion modes that were not considered in the numerical model.

The strong correlation shown in Fig. 12 demonstrates that the numerical model satisfactorily represents the dynamic behavior of a building with roller bearings, and, consequently, the developed methodology is adequate for the analysis of buildings under earthquake excitations.

### 5.2 Parametric study

To assess the performance of seismic isolation, a parametric study was conducted. Thus, the calibrated numerical model of a building with roller bearings was analyzed using six earthquake records.

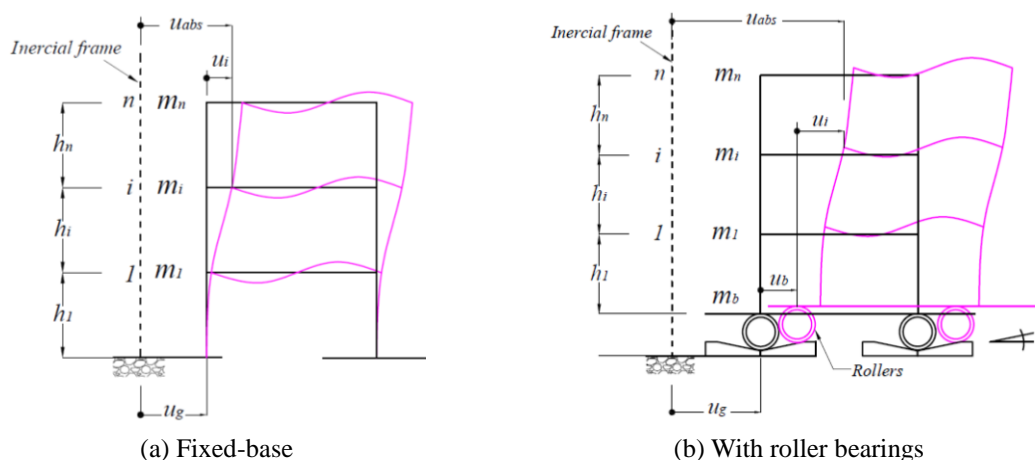


Fig. 13 Displacements of building model

The selection of the records for analysis was based on the classification presented by Naeim and Kelly: (1) excitations with near-fault effects and large ground velocities, (2) high-frequency and high-acceleration excitations and (3) moderate excitations. In this context, a signal representing each group was chosen to analyze the B+RB system. Additionally, the frequency spectra of these signals were expanded by reducing the time step size to excite the modes in a frequency range of 0-50 Hz. The Imperial Valley (El Centro-array #6), Loma Prieta (Corralitos) and Northridge (Century City) earthquakes were used in the seismic analysis. Each of these excitations represents the mentioned groups and were denoted earthquakes one, three and five, while their expanded spectra correspond to earthquakes two, four and six, respectively.

In the first instance, the maximum base displacements ( $u_b$ ), accelerations ( $\ddot{u}$ ) and floor shear forces ( $Q$ ) were determined. To better understand Table 2, a sketch of the two analyzed situations is shown in Fig. 13.

The efficiency of the roller bearings was evaluated through a comparison of the responses of the B+RB system with the responses of the fixed-base building. A variation of the system parameters was obtained (Table 2) whose values represent the seismic response of the B+RB system divided by the seismic response of the fixed-base building. With  $\theta=5^\circ$ , Table 2 shows reductions greater than 50% and 55% in acceleration and shear force, respectively. However, base displacements are excessive in earthquakes one, three and five.

The performance of the roller seismic isolation bearing may be improved by assuming variations in their parameters. The first variation was related to the angle of the sloping surfaces; thus, an angle  $\theta = 2^\circ$  was assumed. Table 2 indicates a slight reduction of base displacement  $u_b$  and an important reduction of story shear with this variation.

The base displacements may be reduced by incorporating energy-dissipation devices, such as sliding surfaces. Assuming a sliding friction force of  $f_{Ds} = 0.8 N$  to ensure the restoring capacity of the system (AASHTO 2000) and  $\theta = 2^\circ$ , the seismic responses listed in Table 2 were obtained. Comparing these results, a slight reduction of base displacement without excessive increase of seismic response is observed, indicating that, as expected, the incorporation of the dissipation system reduces  $u_b$ .

Table 2 Seismic response of buildings with roller isolation bearings

Response	Level	$\theta=5^\circ$						$\theta=2^\circ$						$\theta=2^\circ+$ energy dissipation system					
		Earthquakes						Earthquakes						Earthquakes					
		1	2	3	4	5	6	1	2	3	4	5	6	1	2	3	4	5	6
$u_b$	0	1.91	0.51	1.73	0.47	1.16	0.34	1.64	0.47	1.38	0.31	1.57	0.37	1.45	0.41	1.05	0.28	1.13	0.32
	1	0.49	0.31	0.36	0.20	0.48	0.38	0.19	0.13	0.15	0.10	0.20	0.17	0.25	0.19	0.23	0.12	0.29	0.24
$\ddot{u}$	2	0.24	0.21	0.27	0.10	0.26	0.21	0.12	0.08	0.12	0.04	0.09	0.10	0.13	0.20	0.22	0.06	0.15	0.14
	3	0.22	0.23	0.31	0.08	0.25	0.27	0.09	0.07	0.12	0.04	0.09	0.09	0.12	0.12	0.16	0.05	0.16	0.11
	4	0.36	0.31	0.50	0.12	0.34	0.38	0.13	0.09	0.19	0.06	0.12	0.12	0.15	0.16	0.25	0.07	0.18	0.22
	1	0.15	0.17	0.24	0.06	0.19	0.23	0.07	0.05	0.09	0.03	0.07	0.07	0.09	0.08	0.11	0.03	0.11	0.09
$Q$	2	0.17	0.18	0.28	0.07	0.20	0.25	0.08	0.05	0.10	0.03	0.08	0.08	0.10	0.09	0.13	0.03	0.12	0.10
	3	0.22	0.24	0.35	0.08	0.24	0.31	0.08	0.06	0.14	0.05	0.10	0.10	0.11	0.13	0.16	0.04	0.15	0.14
	4	0.29	0.28	0.45	0.11	0.31	0.36	0.10	0.07	0.17	0.06	0.11	0.11	0.13	0.14	0.21	0.06	0.16	0.19

## 6. Conclusions

This paper presents a numerical and experimental study seeking to validate a model of a building with and without roller seismic isolation bearings subjected to base excitations.

- The modal parameters, FRFs, and acceleration responses numerically obtained are strongly correlated with those obtained experimentally, demonstrating the accuracy of the proposed analysis model. However, it is still possible to improve the correlation, mainly that related to damping ratio.

- In all the earthquakes analyzed, the incorporation of the RB system led to a reduction of the building seismic response, proving that the system is efficient for a large number of seismic excitations.

- In this paper, a simple methodology of numerical analysis of buildings under earthquake excitations was verified through experimental tests. The developed methodology allowed analysis of buildings with RB systems. Assuming a variation in the parameters of the roller seismic isolation bearings, reductions greater than 71% and 79% were achieved in the acceleration responses and shear forces, respectively.

- The results obtained demonstrate that the RB system performs strongly in reduction of the seismic response of buildings under the action of earthquakes. However, buildings with RB systems have excessive base displacements that could limit their design; such problems can be minimized by using energy-dissipation devices.

## Acknowledgments

The authors wish to thank the National Counsel of Technological and Scientific Development (CNPq) for providing financial support and LADEPIS technicians for collaborating in the assembly of experimental tests.

## References

- AASHTO (2000), *Guide Specifications for Seismic Isolation Design*, American Association of State Highway and Transportation Officials, Washington, DC, USA.
- Avallone, E.A and Baumeister, T. (2007), *Marks' Standard Handbook for Mechanical Engineers*, 11th Edition, McGraw-Hill, New York.
- Beijers, C., Noordman, B. and Boer, A. (2004), "A Numerical modeling of rubber vibration isolators: identification of material parameters", *International Congress on Sound and Vibration*, July.
- Bucher, H.F. and Magluta, C. (2011), "Application of joint time-frequency distribution for estimation of time-varying modal damping ratio", *Struct. Eng. Mech.*, **37**(2), 131-148.
- Chung, L.L., Yang, C.Y., Chen, H.M. and Lu, L.Y. (2009), "Dynamic behavior of nonlinear rolling isolation system", *Struct. Control Hlth. Monit.*, **16**, 32-54.
- Gur, S., Mishra, S.K. and Chakraborty, S. (2013), "Performance assessment of buildings isolated by shape-memory-alloy rubber bearing: comparison with elastomeric bearing under near-fault earthquakes", *Struct. Control Hlth. Monit.*, **21**(4), 449-465.
- Jangid, R.S. and Datta T.K. (1995), "Seismic behavior of base-isolated buildings: a state-of-the-art review", *Proc. Inst. Civil Eng. Struct. Build.*, **110**, 186-203.
- Jangid, R.S. and Londhe, Y.B. (1998), "Effectiveness of elliptical rolling rods for base isolation", *J. Struct.*

- Eng.*, **124**(4), 469-472.
- Kunde, M.C. and Jangid, R.S. (2003), "Seismic behavior of isolated bridges: a-state-of-the-art review", *Elec. J. Struct. Eng.*, **3**, 140-170.
- Lee, G.C., Ou, Y.C., Liang, Z., Niu, T. and Song, J. (2007), "Principles and performance of roller seismic isolation bearings for highway bridges", Technical Report MCEER-07-0019, New York, NY, USA.
- Lee, G.C., Ou, Y.C., Niu, T., Song, J. and Liang, Z. (2010), "Characterization of a roller seismic isolation bearing with supplemental energy dissipation for highway bridges", *J. Struct. Eng.*, **136**(5), 502-510.
- Li, Y., Li, J., Li, W. and Samali, B. (2013), "Development and characterization of a magnetorheological elastomer based adaptive seismic isolator", *Smart Mater. Struct.*, **22**(3), 035005.
- Lin, T.W., Chern, C.C. and Hone, C.C. (1995), "Experimental study of base isolation by free rolling rods", *Earthq. Eng. Struct. Dyn.*, **24**, 1645-1650.
- Naeim, F. and Kelly, J.M. (1999), *Design of Seismic Isolated Structures*, Wiley, New York, NY, USA.
- Ou, Y.C., Song, J. and Lee, G.C. (2010), "A parametric study of seismic behavior of roller seismic isolation bearings for highway bridges", *Earthq. Eng. Struct. Dyn.*, **39**, 541-559
- Palazzo, B. and Petti, L. (1999), "Combined control strategy: base isolation and tuned mass damping", *J. Earthq. Technol.*, **36**(2-4), 121-137.
- Rao, P.B. and Jangid, R.S. (2001), "Experimental study of base-isolated structures", *J. Earthq. Technol.*, **38**(1), 1-15.
- Shampine, L.F. and Hosea, M.E. (1996), "Analysis and Implementation of TR-BDF2", *Appl. Numer. Math.*, **20**, 21-31.
- Spencer, Jr. B.F. and Nagarajaiah, S. (2003), "State of the art structural control", *J. Struct. Eng.*, **129**(7), 845-856.
- The Mathworks (2010), The language of technical computing MATLAB.